Molecular Vision 2022; 28:460-479 <http://www.molvis.org/molvis/v28/460>
Received 21 June 2021 | Accepted 19 December 2022 | Published 21 December 2022

Safety evaluation and pharmacodynamics of minocycline hydrochloride eye drops

Xiaoli Li,[1] Wenhua Zhang,[1] Zhiqiang Ye,[2] Shuaili Pei,[2] Dongliang Zheng,[2] Lin Zhu[2]

[1]Henan Eye Institute, Henan Eye Hospital, Henan Provincial People's Hospital, Henan University People's Hospital, Zhengzhou, China; [2]Institute of Advanced Materials for Nano-Bio Applications, School of Ophthalmology & Optometry, Wenzhou Medical University, Wenzhou, China

Purpose: This study evaluated the safe dosage of minocycline hydrochloride (Mino) eye drops and investigated the potential for the prevention or reduction of retinal damage in a diabetic rat model.

Methods: Various concentrations of Mino were applied to human corneal epithelial cells (HCECs) to determine the half maximal inhibitory concentration (IC_{50}). The safety of Mino eye drops was evaluated on Sprague–Dawley (SD) rat eyes by slit-lamp examination, electroretinography (ERG), histology, and TUNEL assay. Eye drops (1 mg/ml) were applied to the streptozotocin-induced diabetic SD rats. Clinical observations, ERG analyses, and optical coherence tomography analyses were performed monthly for five months. Eyes were then analyzed via histology, blood-retinal barrier function assay, and retinal vascular staining.

Results: Cytotoxicity analysis using HCECs revealed that the IC_{50} was 250 μg/ml. Safety analyses in healthy SD rats showed that Mino eye drops did not demonstrate any ocular toxicity. Pharmacodynamics analysis showed that retinal thickness at three months was greater in the Mino group than in the non-treated (NT) group. The peak times and amplitudes of each program were better in the Mino group than in the NT group at each time point by ERG analyses. Histology examina-tions showed a thinner ganglion cell layer, fewer ganglion cells, and more dilated blood vessels in the NT group than in the Mino group.

Conclusion: Mino eye drops at 1 mg/ml were safe when used in SD rats. Mino eye drops can protect the retina from the development or progression of diabetic retinopathy.

Diabetic retinopathy (DR) is a common complication of diabetes; its incidence increases progressively with age and impacts on the quality of people's lives. Research regarding DR is important because of its high incidence, long disease course, and difficult management. Retinal laser photocoagulation, intravitreal injection of anti-vascular endothelial growth factor (VEGF), and vitrectomy are major forms of treatment; however, these three methods are invasive. Thus, there is a need to develop a non-invasive method to manage DR or delay its progression.

Because of its anti-inflammatory, anti-apoptotic, and anti-microglia activation effects, minocycline (Mino) has been investigated for the treatment of DR; it reportedly exhibits retinoprotective effects against DR. Recently, Stephanie et al. [1] reported that Mino significantly reduced retinal apoptosis in type 1 db/+ streptozotocin (STZ)-induced diabetes mice, similar to the effects of insulin administration. Krady et al. [2] reported that Mino reduced proinflammatory cytokine expression, microglial activation, and caspase-3 activation in a rodent model of DR. Chen et al. [3] found that Mino activated the TXNIP/NLRP3 inflammasome pathway, which contributes to inflammation in diabetic retinopathy. Jason et al. [4] showed that Mino prevented diabetes-related degeneration of retinal capillaries by inhibiting caspase-1/IL-1β signaling. A phase I/II clinical study in the United States (NCT01120899) suggested that oral Mino was effective in the treatment of diabetic macular edema [5].

However, studies regarding Mino treatment for DR have used systemic administration methods alone (e.g., oral administration in humans and intraperitoneal injection [IP] in animals); to the best of our knowledge, no report has described the local administration (eye drops or intraocular injection) of Mino. Compared with systemic administration, local administration reduces the blood concentration of the drug and avoids drug-related organ damage. Mino exhibits hepatotoxicity and nephrotoxicity, especially in patients with diabetes who have kidney injuries. However, Mino is considered safe for short-term use in dermatology and ophthalmology applications; topical administration is preferred because it causes minimal systemic effects. Thus, there is a need to investigate the safety and efficacy of locally administered Mino. This study evaluated the safe dosage of

Correspondence to: Lin Zhu, Institute of Advanced Materials for Nano-Bio Applications, School of Ophthalmology & Optometry, Wenzhou Medical University, Wenzhou, China; Phone: 057788067973; FAX: 057788067973; email: linzhudai123@hotmail.com

Mino eye drops and investigated the potential for the prevention or reduction of retinal damage in a diabetic rat model.

METHODS

HCEC cytotoxicity analysis:

Live/dead assay—The in vitro cytotoxicities of various concentrations of Mino against human corneal epithelial cells (HCECs) were determined by the live/dead assay, using calcein-AM and propidium iodide (PI) staining. Cells were seeded at a density of 4×10^4 cells/well (n = 6 wells per concentration) in 24-well plates and incubated for 24 h in a CO_2 incubator at 37 °C. Various concentrations of Mino were added to the wells to achieve final drug concentrations ranging from 0.116 to 1106 μg/ml. After 48 h of incubation, 200 μl of calcein-AM (2 μmol/l) and PI (4 μmol/l) solution were added, and the cells were incubated for an additional 15 min. Finally, living and dead cells were observed and photographed at 490 nm and 535 nm, respectively, using a fluorescence microscope (IX81, Olympus, Japan). Untreated cells were used as controls.

CCK-8 assay—The half maximal inhibitory concentration (IC_{50}) of Mino that elicited a response in HCECs was determined by the cell counting kit-8 (CCK-8) assay. Cells were seeded at a density of 7×10^3 cells/well (n = 6 wells per concentration) in 96-well plates and incubated for 24 h in a CO_2 incubator at 37 °C. Various concentrations of Mino solution were added to the wells to achieve final drug concentrations identical to the concentrations in the live/dead assay. After 24 h or 48 h of incubation, the culture medium was replaced with 200 μl of culture medium containing 10% CCK-8 solution (PH1759, DPBS Phygene, Fuzhou, China), and the cells were incubated for an additional 2 h. Finally, absorbance was determined at 450 nm using a microplate reader (Model SpectraMax M5, Molecular Devices, CA). Untreated cells were used as controls. Cell viability was calculated using the following equation: Cell viability (%) = absorbance of tested sample/absorbance of control sample × 100. All experiments were performed in triplicate. The cell viability results were used to determine the IC_{50} of Mino, which elicited a response in HCECs.

Preparation and characteristics of Mino eye drops: To identify the proper solvent for Mino eye drops, we measured the drug concentration of the saturated solution using each of three solvents: phosphate-buffered solution (PBS), Dulbecco's phosphate-buffered saline (DPBS), and normal saline. We prepared the three saturated solutions of Mino in the above three solvents and used high-pressure liquid chromatography (HPLC; Agilent 1200, Agilent, CA) to measure the saturated concentrations.

Cell viability analysis indicated that the IC_{50} of Mino in HCECs was 250 μg/ml. We established three separate concentrations (250, 500, and 1000 μg/ml) of Mino with PBS or normal saline as solvent; we measured the pH values of these solutions using a pH meter (SG2, Mettler Toledo, Germany).

Safety evaluation of Mino eye drops in SD rats:

Animals and groups—Twelve adult male SD rats weighing between 250 g and 300 g were used in this experiment. A slit-lamp examination was used to observe the anterior segment and confirm the presence of a healthy eye surface. Using PBS as a solvent, we prepared three concentrations of Mino eye drops.

The rats were randomly divided into four groups: high concentration, middle concentration, low concentration, and blank control (n = 3 rats per group). The right eyes of the animals in each group were administered Mino or blank PBS eye drops (one drop, three times daily) for two weeks. During the administration of eye drops, the head of each rat was fixed to maintain the eye drops on the eye surface for 30 s, thereby avoiding drug loss caused by blinking.

Slit-lamp examination—On the first, third, seventh, and 14th days after beginning the eye drop administration, the anterior segment of each eye was inspected via slit-lamp examination, and conjunctival congestion was scored as follows: no congestion, 0; mild congestion, 1; moderate congestion, 2; and severe congestion, 3. The cornea was then stained and observed with a fluorescein sodium staining strip to determine whether cornea impairment was present.

Full-field electroretinography (ERG)—On the seventh and 14th days after beginning the eye drop administration, all rats underwent full-field ERGs to evaluate retinal function, using the RETIport system with a custom-built Ganzfeld dome (Roland Consult, Wiesbaden, Germany). The pupils of the animals were dilated with a single drop of 0.5% tropicamide and 0.5% phenylephrine solution (Santen Pharmaceutical Co., Ltd., Osaka, Japan), then dark-adapted for 2 h. Under dim red light, the animals were anesthetized via an intramuscular injection of 2% pentobarbital sodium (40 mg/kg bodyweight). A small amount of 2.5% methylcellulose gel was then applied to each eye, and a rat-optimized copper loop electrode was placed on the cornea to record the ERGs. The needle reference and ground electrodes were inserted into the cheek and tail, respectively. Dark-adapted ERG responses were recorded, including a rod response (dark-adapted 0.01 ERG), standard combined ERG (dark-adapted 3.0 ERG), and oscillatory potentials (OPs). Thereafter, the animals were

light-adapted for 5 min under a light intensity of 25 cd/m^2; light-adapted ERG responses were recorded, including a cone response (light-adapted 3.0 ERG) and 30-Hz flicker. For each of the five stimulus programs, the mean amplitudes and implicit times were recorded and analyzed for each group.

Histology and TUNEL assay—On the 14th day after beginning the eye drop administration, all animals were euthanized under deep anesthesia. The eyeballs were quickly removed and fixed in 4% paraformaldehyde for 24 h. One half of each eye wall was embedded in paraffin wax and dissected vertically in 5-μm-thick serial sections, which were stained with hematoxylin and eosin (HE) and observed with an optical microscope (IX81, Olympus).

The other half of each eye wall was embedded in OCT medium for frozen-section terminal deoxynucleotidyl-transferase-mediated biotin-dUTP nick-end labeling (TUNEL) assay analysis. The eyeball wall was serially cryosectioned vertically at a thickness of 10–12 μm. Six sections of each animal eye were subjected to TUNEL assay using the TUNEL Apoptosis Detection Kit Version 2.0 (PH1731, Phygene Life Science, China) in accordance with the manufacturer's instructions. Images of the corneas were acquired using an optical microscope (IX81, Olympus). The quantities of apoptotic cells in the sections of the whole cornea were manually counted in a blinded manner and then subjected to statistical analysis.

Pharmacodynamics of Mino eye drops in streptozotocin (STZ)-induced diabetic SD rats:

Diabetic SD rat model—Thirty adult female SD rats weighing 250 ± 10 g were used for the preparation of STZ-induced diabetes. Biomicroscopy examinations showed that none of the rats had oculopathy, and all of the rats had a blood glucose < 8.89 mmol/L. All rats fasted for 12 h before treatment with STZ; their weights and blood glucose levels were also recorded before treatment. Twenty of the 30 rats received IP STZ at a dose of 55 mg/kg bodyweight. The remaining 10 rats (blank control group) were injected with the same volume of blank sodium citrate buffer. At 1, 3, and 7 days after injection, weights and blood glucose levels were recorded, and the successful establishment of diabetes was defined as a consistent blood glucose level > 13.0 mmol/l. Importantly, one of 10 rats in the Mino group and one of 10 rats in the non-treated group died of poor general conditions during the study.

Blood glucose and bodyweight were measured at intervals of two weeks throughout the experiment to ensure that blood glucose levels in diabetic rats remained > 13.0 mmol/L. After confirmation of the diabetic model establishment (i.e., beginning on the seventh day after IP injection), the right eyes of 10 diabetic rats were treated with Mino eye drops (one drop, three times daily; Mino group). The right eyes of the remaining 10 diabetic rats and 10 non-diabetic rats were treated with blank PBS eye drops (non-treated [NT] and control groups, respectively).

Slit-lamp and funduscopic examinations—At 4, 8, 12, and 16 weeks after beginning the eye drop administration, all rats were observed under a slit-lamp microscope by a professional to identify any complications. All rats also underwent funduscopic examinations by another professional, and the fundus vessel condition was recorded.

Full-field ERG—All rats underwent ERG examinations at 1, 2, 3, and 4 months after beginning the eye drop administration, using the method described in Section 2.3.3 above.

Optical coherence tomography (OCT): All rats underwent OCT examinations at 1, 2, and 3 months after beginning the eye drop administration; however, some rats could not be examined because of diabetic cataracts. The OCT examination method followed a previously published protocol [6]. Briefly, x-axis scanning (from right to left) and y-axis scanning (from bottom to top) were performed, as shown in Figure 1. For x-axis scanning, the OCT system first identified the optic nerve head on the computer screen and then scanned from 9 o'clock to 3 o'clock, crossing the optic nerve head (Figure 1B). Next, the OCT system was scanned horizontally at distances of half the papilla above and below the optic nerve head (Figure 1A–C). For y-axis scanning, the OCT system first identified the optic nerve head on the computer screen and then scanned from 6 o'clock to 12 o'clock, crossing the optic nerve head (Figure 1E). Next, was scanned vertically by OCT at distances of half the papillary diameter (PD) above and below the optic nerve head (Figure 1D,F). All images were generated by 100 scans. Two or three points in each image were selected to measure retinal thickness using ImageJ software. In Figure 1B,E, two points (Points d, e, k, and i) in each figure were selected at distances of 1 mm from the center of the optic nerve head. In Figure 1A,C,D,F, three points in each figure were selected, as shown. Overall, the retinal thickness and distance from the retinal pigment epithelium layer (RPEL) to the inner membrane layer (INL) were measured at 16 points in each eye using ImageJ software; at these 16 points, the ganglion cell inner plexiform layer (GCIPL) and distance from INL to the inner cluster layer (ICL) were also measured. The mean retinal thickness of a single rat eye was regarded as the mean thickness of these 16 points. Finally, the differences in measurement results among the three groups were assessed by statistical analysis.

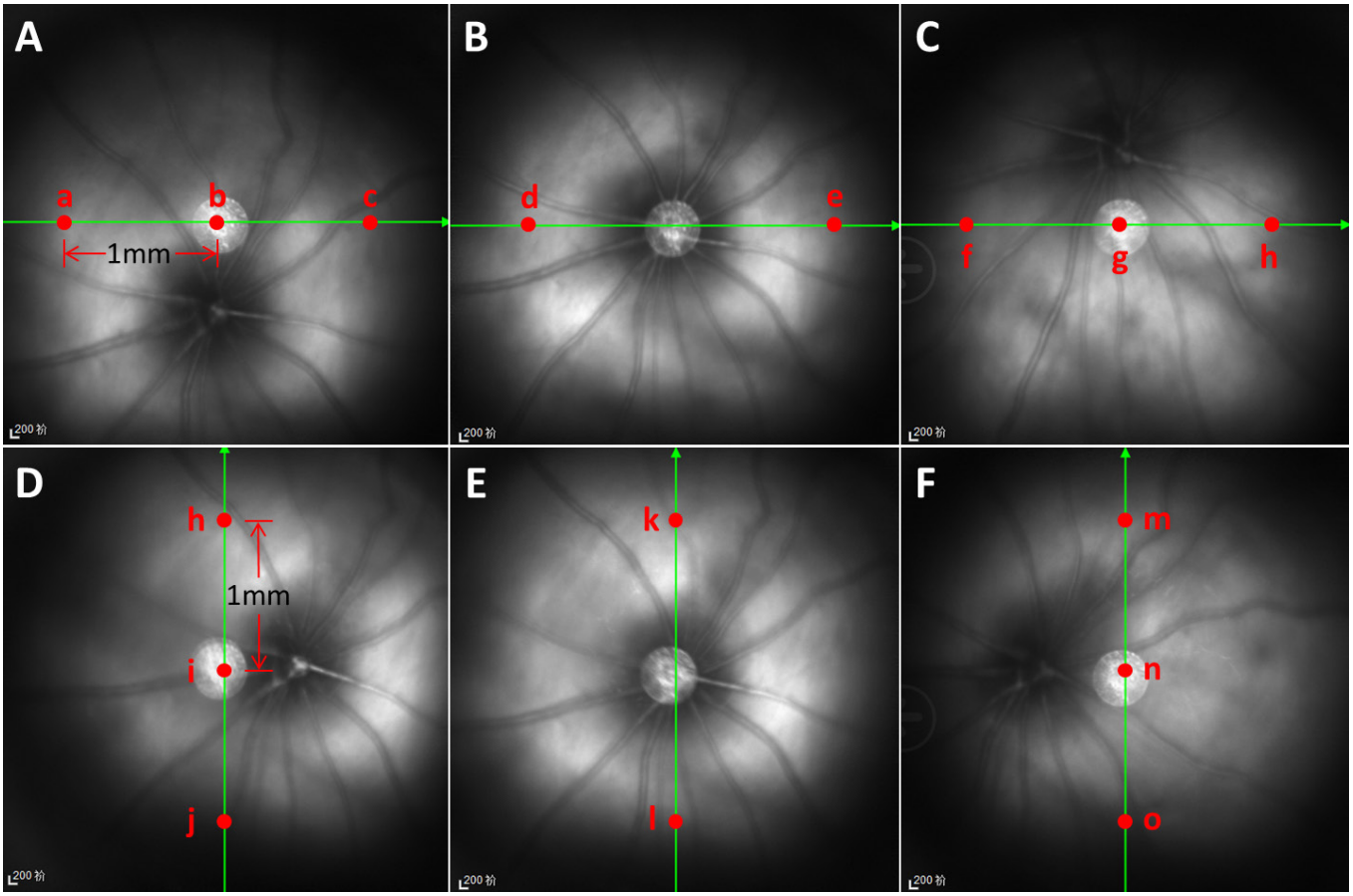

Figure 1. Retina scanning positions and retinal thickness measurements during OCT examination. Panels **A**–**C** show scanning images of the x-axis; panels **D**–**F** show scanning images of the y-axis. **B** and **E** show x-axis and y-axis OCT scanning through the discus opticus alone. **A** and **C** show x-axis scanning at a distance of 0.5 PD upwards and downwards from the discus opticus. **D** and **F** show y-axis scanning at a distance of 0.5 PD rightward and leftward from the discus opticus. Red points indicate the locations at which the retinal thickness was measured.

Histology: At 20 weeks after beginning the eye drop administration, three rats were randomly selected from each group and euthanized with an anesthesia overdose. Their eyeballs were carefully removed, fixed in a special fixative solution, dehydrated using a graded ethanol series, embedded in paraffin, sectioned at a thickness of 5 μm, and stained with hematoxylin and eosin using the method described in Section 2.3.4 above.

Evans blue assay: At 20 weeks after beginning the eye drop administration, Evans blue assays were performed to evaluate retinal vascular permeability. This assay comprised Evans blue staining of rat blood vessels to observe retinal vascular permeability, as well as quantification of Evans blue content in retinal tissue to characterize blood retinal barrier (BRB) permeability.

For Evans blue staining of rat blood vessels, three rats were randomly selected from each group and anesthetized in a routine manner; Evans blue (45 mg/kg) was slowly injected into the jugular vein of each rat. When a rat's eyes, mouth, and limbs exhibited a blue color, the rat was sacrificed by cervical dislocation. The eyeballs were removed and fixed in 4% paraformaldehyde for 12 h. The whole retina was then separated and carefully stretched. Flat-mounted retinas were observed and photographed under a fluorescence microscope.

For quantification of Evans blue content in retinal tissue, the remaining three rats were randomly selected from each group and anesthetized in a routine manner. Evans blue (45 mg/kg) was slowly injected into the jugular vein of each rat. After 2 h of staining, 1% paraformaldehyde was perfused into each rat's left ventricle. The eyeball was removed after paraformaldehyde circulation for 3 min, and the retinal tissue of each eyeball was collected with the aid of a surgical microscope. The tissue was dried at 4 °C, then weighed, using an electronic balance and incubated with 150 μl formamide at

70 °C for 18 h. Finally, it was centrifuged at 12,000 r/min for 2 min at 4 °C. The absorbance values of the samples were measured with an enzyme labeling instrument at wavelengths of 620 nm and 740 nm. The concentration of Evans blue in the retinal tissue was calculated with the following standard curve equation: y = 0.02136 × -1.8955, where y is the relative absorptivity and x is the concentration (mg/ml) of Evans blue.

Statistical analysis: All data were expressed as means ± standard deviations; they were analyzed using SPSS Statistics for Windows (version 20.0, IBM Corp., New York, NY). For the CCK-8 results, ERG, and retinal thickness (determined by both HE staining and OCT), a multi-factor ANOVA was used to evaluate the influences of time and group on the results. For Evans blue assays, a one-way ANOVA was used to compare differences among the groups. Differences with $p < 0.05$ were considered statistically significant.

RESULTS

IC_{50} of Mino responses to HCECs: Figure 2 shows the results of live/dead staining to determine the effects of Mino concentration on HCEC growth. Compared with the control group, a drug concentration > 35 μg/ml led to cell death in HCECs. Drug concentrations < 35 μg/ml did not affect HCEC growth.

The CCK8 assay findings were consistent with the results of live/dead staining. As shown in Figure 3, drug concentrations < 35 μg/ml permitted ≥ 80% cell activity in HCECs at 24 h and 48 h. Drug concentrations > 35 μg/ml led to decreasing cell activity in HCECs, in a manner that was amplified by increasing drug concentration. At a drug concentration of 1106 μg/ml, cell activities in HCECs at 24 h and 48 h were 10.23 ± 0.39% and 5.25 ± 0.67%, respectively, which suggested severe inhibition. The drug concentration-cell

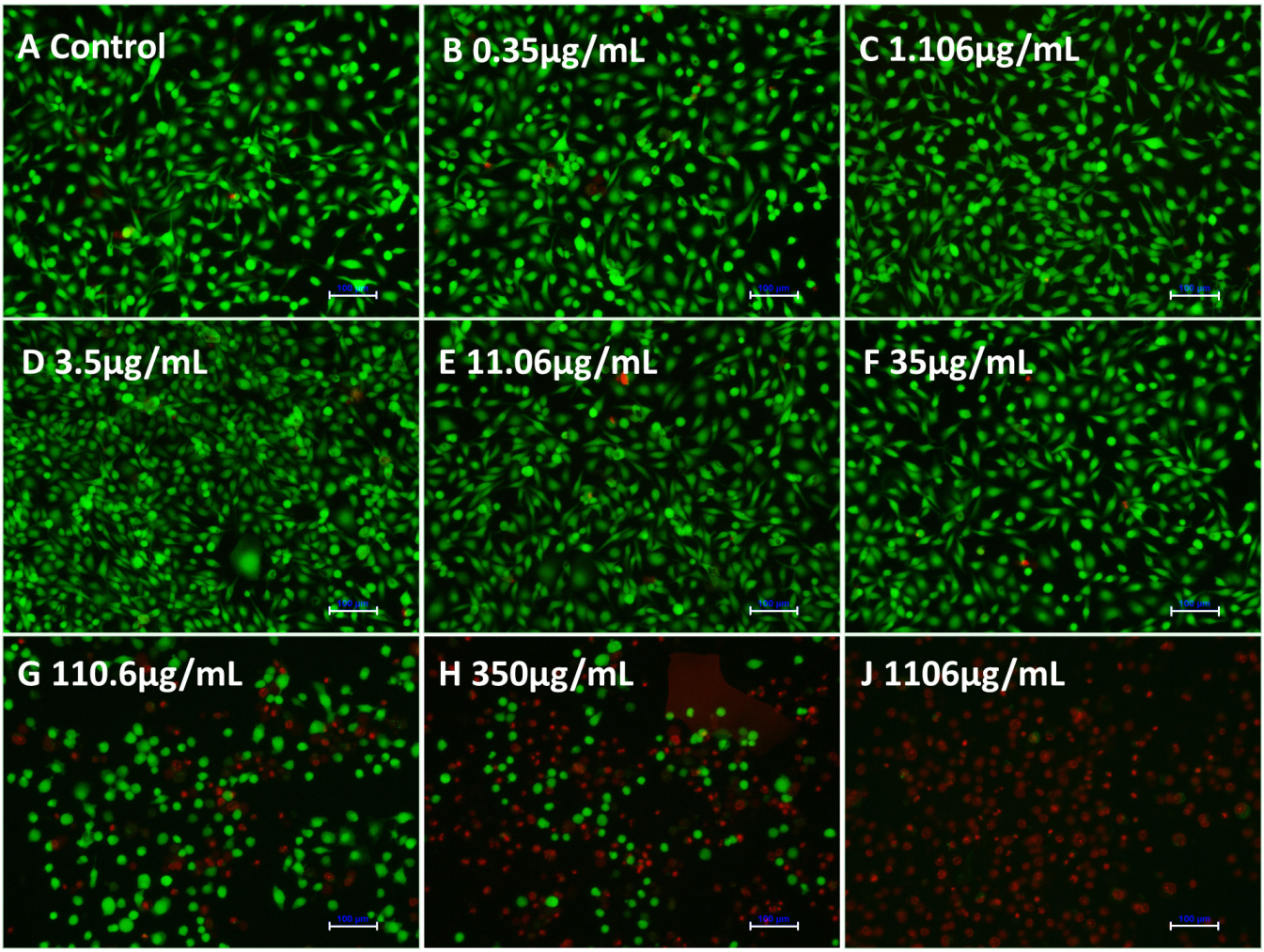

Figure 2. Live/dead staining of HCECs after co-culture with various concentrations of minocycline hydrochloride (Mino) for 24 h**.** Green staining indicates calcein-AM, and red staining indicates propidium iodide (PI). Scale bar: 100 μm.

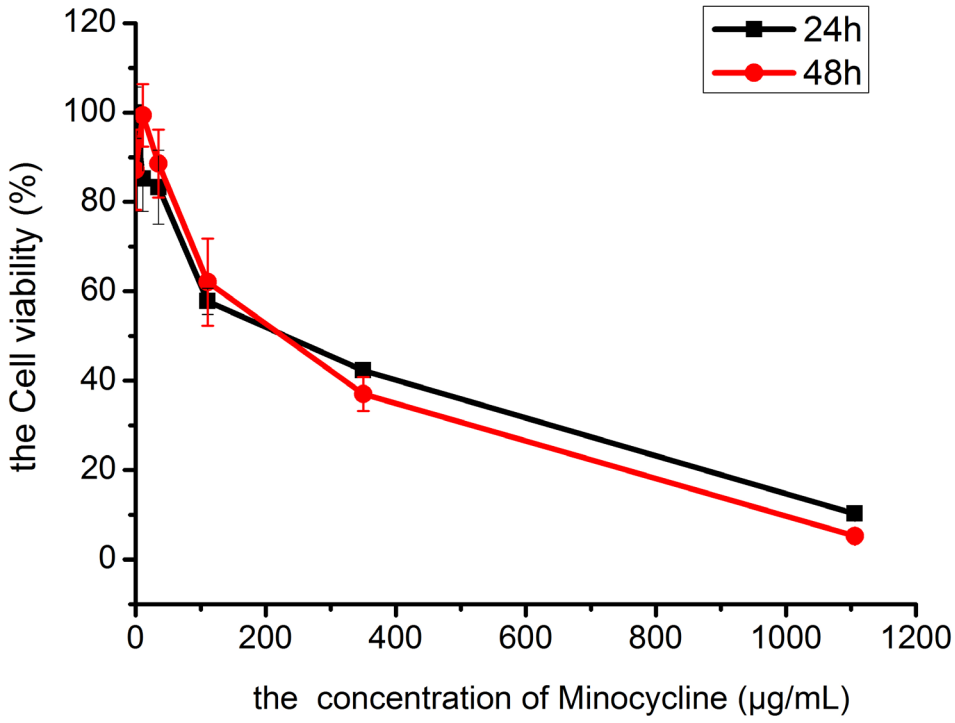

Figure 3. Drug concentration–cell viability curves of HCECs compared among drug concentrations.

activity curve (Figure 3) indicated that the IC_{50} of Mino that elicited a response in HCECs was 250 μg/ml.

Solvent for Mino eye drops: Table 1 shows the saturated drug concentrations of Mino in various solvents. Compared with DPBS and normal saline, the solubility of Mino was highest in PBS (6.79 ± 0.42 mg/ml). Table 2 shows the pH values of the Mino solution at different concentrations in normal saline and PBS. Compared with normal saline, the pH values of Mino in PBS were closer to the pH of human body fluid (7.3–7.4). Therefore, PBS was selected as the solvent for Mino eye drops in our animal experiments.

Mino eye drop safety in SD rats: As shown in Figure 4, rats in the high, middle, and low concentration groups showed no conjunctival congestion, circuitous blood vessels, or changes in retinal thickness after 1–14 days of eye drop treatment. Moreover, they showed no corneal opacification, anterior chamber cells, lens opacification, iris synechiae, iris vessel thickening, or iris vessel thinning. The fluorescein sodium staining photos of the cornea are shown in Figure 5.

The ERG examinations showed that all indices in the high, middle, and low concentration groups (Table 3) did not significantly differ from indices in the control group, which suggested that Mino eye drops at 250–1000 μg/ml were non-toxic for rat retinas over an interval of two weeks. Histological analysis showed no corneal pathology in any of the experimental groups. Figure 6A shows the corneal HE staining in the high concentration group at two weeks after beginning the eye drop administration. TUNEL assay analysis showed no obvious apoptotic cells in the corneas of any rat, which suggested that Mino eye drops at 250–1000 μg/ml did not damage the rat cornea. Figure 6C shows the corneal TUNEL

Table 1. Saturated drug concentrations of minocycline hydrochloride in various solvents.

Solvent	Solubility (mg/ml)
DPBS	3.65±0.05
PBS	6.79±0.42
Normal saline	2.24±0.35
ddH_2O	7.41±0.29

DPBS: Dulbecco's phosphate-buffered saline; PBS: phosphate-buffered saline; ddH_2O: double distilled water

Table 2. pH values of minocycline hydrochloride solutions at various concentrations in normal saline and PBS.

Group	Drug concentration	Normal saline	PBS
Control group	Blank	6.25±0.03	7.47±0.02
1 × IC_{50}	250 μg/ml	4.47±0.02	7.37±0.01
2 × IC_{50}	500 μg/ml	4.17±0.03	7.28±0.01
4 × IC_{50}	1000 μg/ml	4.09±0.01	6.89±0.03

PBS: phosphate-buffered saline; IC_{50}: half maximal inhibitory concentration.

staining in the high concentration group at two weeks after beginning the eye drop administration.

Use of Mino eye drops to protect rat retinas from the development or progression of DR: Figure 7A shows that the blood glucose in the experimental group increased rapidly after an IP injection of STZ. Throughout the experiment, all blood glucose values in the experimental group were > 13 mmol/l and exhibited an upward tendency, which indicated that the diabetic rat model had been successfully established. Conversely, the blood glucose values in the control group were < 13 mmol/L and generally stable. Figure 7B shows that the mean weights were similar among the groups at baseline. After an IP injection of STZ, the weight of the rats in the experimental groups decreased over time, while the weight of the rats in the control group gradually increased. These blood glucose and bodyweight findings suggest the successful establishment of a diabetic rat model.

Figure 8A,B shows slit-lamp examination findings of gradual cataract onset in diabetic rats one month after the IP injection of STZ. Because cataracts were not scored in this experiment, we did not investigate differences in the degree of cataracts between the NT and Mino groups. During slit-lamp examination observation and follow-up, we found some abnormalities in the iris vessels of diabetic rats (e.g., proliferation, changes in thickness, tortuosity, and/or bead-like alterations; Figure 8C,D). These findings suggest potential changes in the ocular and retinal blood vessels in diabetic rats.

Table 4 shows the mean retinal thicknesses, as measured by OCT, at 1, 2, and 3 months after beginning the eye drop administration. The mean thicknesses of the overall retina and the GCIPL of the right eyes in the Mino group were thicker than those values in the fellow eyes at each time point, and thicker than the values in the NT group at each time point. The overall retinal thickness and GCIPL thickness differed among the three groups according to the ANOVA findings. However, there were no significant differences in overall retinal thickness and GCIPL thickness between the Mino and NT groups. Finally, the overall retinal thickness and GCIPL thickness in the diabetic rats gradually decreased.

Table 5 shows the ERG findings at 1, 2, 3, and 4 months after beginning the eye drop administration. All wave amplitudes of each ERG program were lower in the experimental groups than in the blank control group; these differences gradually increased. These results suggested that the retinal function was damaged in diabetic rats, and that this damage gradually increased. In addition, the P-N wave amplitude of the flash ERG was significantly different between the Mino and NT groups ($p = 0.013$). Other ERG findings between the Mino and NT groups did not show significant differences.

Figure 9 shows the retinal HE staining images of each group at four months after beginning the eye drop administration. The structure of the retinal layers in the blank control group was clear, and the morphology was normal (Figure 9A). In the NT group, the structure of the retinal layers was disordered; the ganglion cell layer was thinner and contained fewer ganglion cells; and the inner nuclear layer exhibited swelling of retinal cells, infiltration of inflammatory cells, and obvious dilatation of blood vessels (Figure 9B). In the right eye (Figure 9C) and fellow eye (Figure 9D) of the Mino group, the retinal structure was ordered without inflammatory cells or vascular dilatation; moreover, the cells exhibited regular arrangement and significantly more ganglion cells compared with the NT group.

As shown in Figure 10, the contents of Evans blue in the retinal tissue of the blank control group, right eye of the Mino group, fellow eye of the Mino group, and right eye of the NT group were 1.56 ±0.12 μg/mg, 4.57 ± 0.76 μg/mg, 5.00 ±0.66 μg/mg, and 6.98 ± 0.82 μg/mg, respectively. These results showed that Mino inhibited BRB permeability in diabetic rats. Furthermore, the retinal blood vessels of the diabetic rats were tortuous, proliferated, thickened, and leaked fluorescent dye in the NT group (Figure 11A), which indicated damage to the BRBs. In the blank control group, the morphology of the retinal blood vessels was intact, with uniform dye distribution and no obvious leakage. In the right

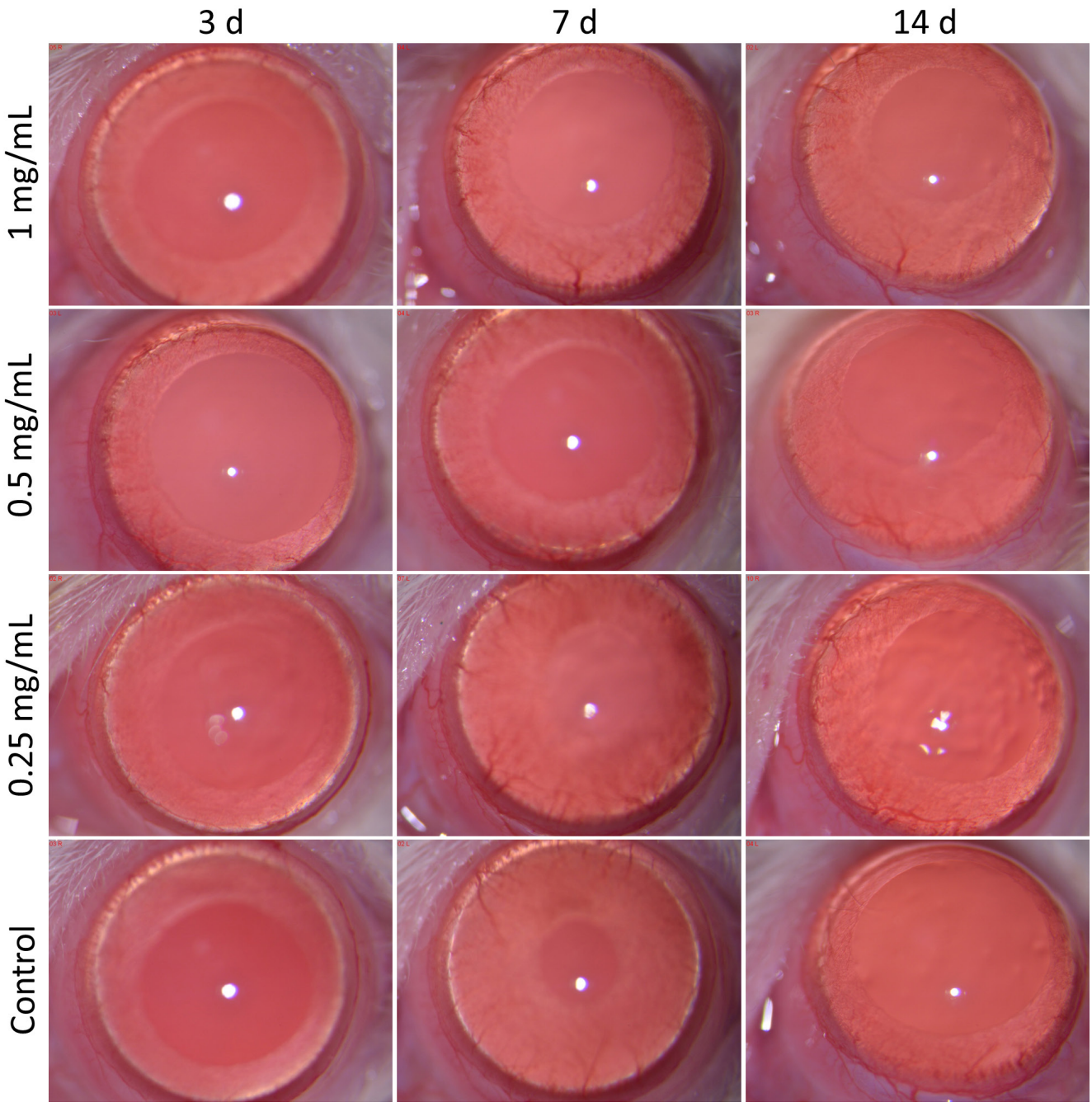

Figure 4. Photos of rat eye anterior segment in all groups under slit-lamp examination at 1, 3, 7, and 14 days after beginning the eye drop administration.

eye of the Mino group, some vessel dilatation was present, but no obvious vascular leakage was evident (Figure 11B).

DISCUSSION

Safe dose of Mino in corneal epithelial cells: Mino is a commonly used antibiotic that is mainly administered orally or intravenously. The mean drug concentration in the serum was reportedly 3.5 μg/ml at 1 h after the oral or intravenous administration of Mino 200 mg [7]. Therefore, we presumed

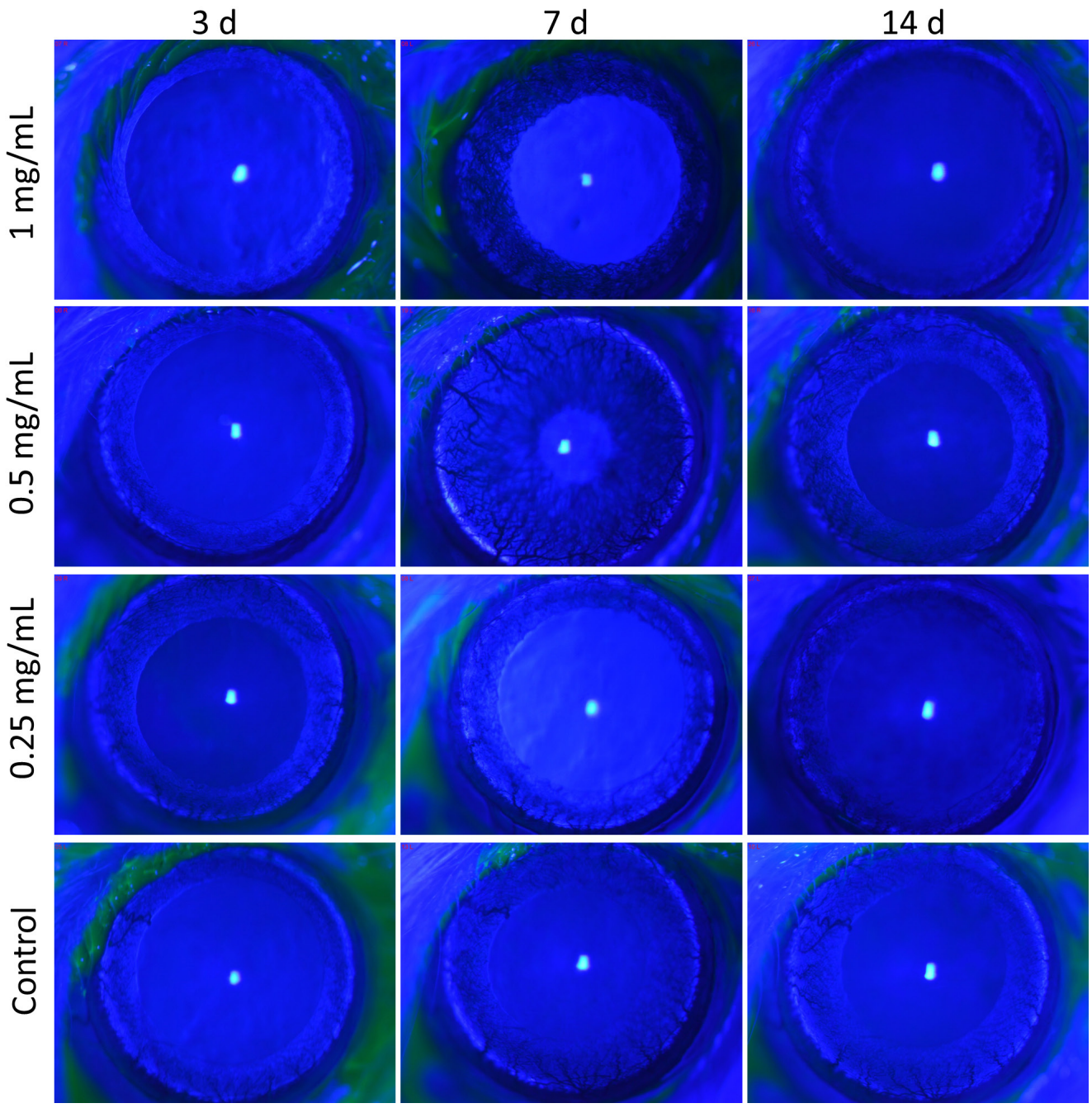

Figure 5. Fluorescein sodium staining photos of rat corneas in all groups under slit-lamp examination at 1, 3, 7, and 14 days after beginning the eye drop administration.

that 3.5 μg/ml of Mino is a safe drug concentration for the human body. Using this drug concentration in our cell experiments, we increased and decreased the drug concentration in a gradient manner to identify the minimum safe concentration of Mino for HCECs and calculated its median lethal concentration. Hollborn [8] reported that Mino at low concentrations (i.e., 22.87 ng/ml to 9.15 μg/ml) stimulated chemotaxis and decreased the proliferation of retinal pigment epithelium (RPE) cells, while Mino at concentrations above 9.15 μg/ml decreased the viability of RPE cells by inducing cell necrosis. Our results showed that the cell viabilities of HCECs at 24 h and 48 h were > 80% when the drug concentration was < 35 μg/ml, which differed from the findings in RPE cells.

Table 3. Results of each ERG program at 1 and 2 weeks after administration of eye drops.

Program	Time	Wave	High concentration group	Middle concentration group	Low concentration group	Control group
Dark-adapted 0.01 ERG	1 w	b-wave (μV)	101.08±24.61	78.93±30.49	88.27±17.22	107.87±35.92
	2 w	b-wave (μV)	98.89±42.68	83.74±28.84	78.53±34.94	85.78±41.19
Dark-adapted 3.0 ERG	1 w	a-wave (μV)	41.47±7.89	43.28±3.43	53.12±13.21	50.63±16.95
		b-wave (μV)	101.95±21.96	115.48±20.35	140.18±48.87	148.41±47.22
	2 w	a-wave (μV)	43.71±9.12	57.52±10.48	40.63±7.46	43.00±11.06
		b-wave (μV)	131.00±35.87	148.00±24.36	107.50±31.17	124.31±34.49
Dark-adapted 3.0 oscillatory potential	1 w	OS_2 (μV)	67.62±31.51	70.15±19.01	74.76±50.03	71.12±29.06
	2 w	OS_2 (μV)	47.80±11.31	77.62±27.40	39.63±24.04	51.34±24.97
Light-adapted 3.0 ERG	1 w	a-wave (μV)	2.78±0.76	5.85±4.76	3.67±0.95	2.15±1.76
		b-wave (μV)	19.00±11.99	22.68±4.70	24.50±11.96	22.13±6.45
	2 w	a-wave (μV)	3.73±1.32	3.57±1.52	3.37±1.52	2.82±1.90
		b-wave (μV)	18.50±5.08	22.84±7.26	19.74±4.45	20.00±6.77
Light-adapted Fare ERG	1 w	P1-N1 (ms)	15.68±2.47	18.28±2.59	16.36±2.02	16.64±1.61
		P1-N1 (μV)	5.80±1.55	6.18±2.76	7.43±1.76	5.94±1.99
	2 w	P1-N1 (ms)	18.31±3.16	16.06±2.92	17.47±4.39	18.38±3.64
		P1-N1 (μV)	4.60±1.40	4.75±1.29	7.51±2.30	5.22±1.66

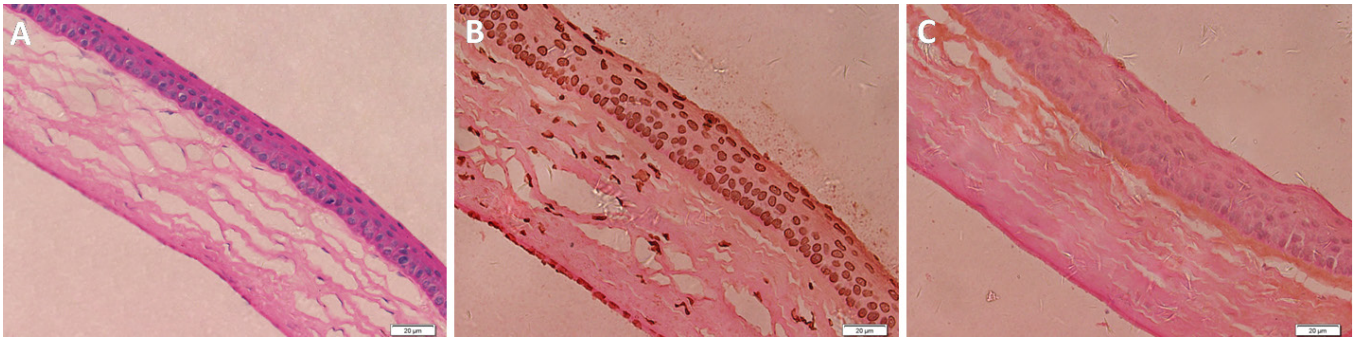

Figure 6. Corneal HE staining and TUNEL staining in the high concentration group at two weeks after beginning the eye drop administration. **A**: Corneal HE staining; **B**: Positive control of TUNEL staining; **C**: Negative control of TUNEL staining.

Notably, RPE cells are more sensitive than HCECs; therefore, the tolerable drug concentration is lower for RPE cells.

Selection of solvent for Mino eye drops: Mino has strong polarity and can dissolve in water; its hydrochloride salt, minocycline hydrochloride, has greater solubility in water. Our results showed that the saturation solubility of Mino in normal saline was 2.24 ± 0.35 mg/ml, while its saturation solubility in PBS was 6.79 ± 0.42 mg/mL; these findings might be influenced by the ionic strength and pH in PBS. When PBS was the solvent, the pH value of the solution decreased with increasing drug concentrations. The pH value changed comparatively little in PBS because of the solvent buffering action, and remained closer to the pH value of the human body compared with normal saline. Therefore, we selected PBS as the solvent in the animal experiments.

Retinal entry of Mino eye drops in DR rats: Topical delivery is a commonly used and non-invasive method for treating ophthalmic diseases. Productive absorption from topical delivery to the posterior segment occurs via corneal and non-corneal (conjunctival/scleral) pathways [9]. In the corneal pathway, the drug gradually diffuses the posterior segment by moving down a concentration gradient, which leads to a decrease in drug concentration. Less than 3% of the drug passes through the cornea into the anterior chamber [10]; the drug concentration further decreases with the circulating flow of aqueous humor. However, pigment in the iris can bind to the drug, which increases the content of the drug in the eye. The drug can spread to the iris root and posterior chamber and then reach the posterior segment. Furthermore, diabetic patients exhibit pathological changes in the cornea [11]: accumulation of glycogen granules in the epithelium, occasional focal degeneration of epithelial cells, irregular thickening of the epithelial basement membrane, and multilamination. These pathological changes might allow small molecules to enter the cornea.

In the non-corneal pathway, blood flow from the conjunctiva and choroid transports some drugs into systemic circulation and causes drug loss. Some other proportions of drugs pass through the pars plana into the posterior segment and avoid the BRB [12]. In this process, the dense collagen fiber of the sclera is an important anatomic barrier that prevents drug entry into the vitreous. The rat sclera is thinner than the human sclera, and in vitro experiments have shown that scleral permeability to a particular drug is inversely proportional to scleral thickness [13]. Therefore, a drug can reach the posterior segment more easily in rats than in humans. We tested three drug concentrations of Mino drops as ophthalmic treatments for rats and found no obvious abnormalities, which suggested that the dosage and topical delivery method were safe for the rat retina.

Our in vitro findings indicated that the LC_{50} of Mino in HCECs was 250 μg/ml. There are notable differences between in vivo and in vitro conditions. In particular, tear circulation and metabolism after topical delivery lead to short drug persistence in the cornea. Furthermore, the lacrimal film reduces drug entry into corneal endothelial cells. We established three comparatively high drug concentrations in vivo to evaluate the safety of Mino administered topically. Importantly, no concentrations were associated with substantial retinal abnormalities; thus, we selected the highest dose (1000 μg/ml) for pharmacodynamic analysis to improve intraocular drug concentration. Although we did not conduct an in vivo pharmacokinetics analysis, the pharmacodynamic findings indicated that topically administered Mino could delay DR development, suggesting that 1000 μg/ml Mino can enter the retina in DR rats.

Mino eye drops can effectively delay the occurrence of DR: We used ERG, OCT, histological analysis, and Evans blue staining to evaluate the effects of topical delivery of Mino on DR. A sensitive means of assessing retinal function, ERG

has been used in clinical examinations [14] and basic research regarding DR. Li et al. [15] reported that the ERG responses of STZ-induced diabetic rats were reduced in a-wave and b-wave amplitudes within two weeks after the onset of diabetes. Aizu et al. [16] reported that the a-wave and b-wave amplitudes and OPs were reduced in BN rats one month after the onset of STZ-induced diabetes. Malechka et al. [17] demonstrated that light-adapted and dark-adapted a-wave and b-wave

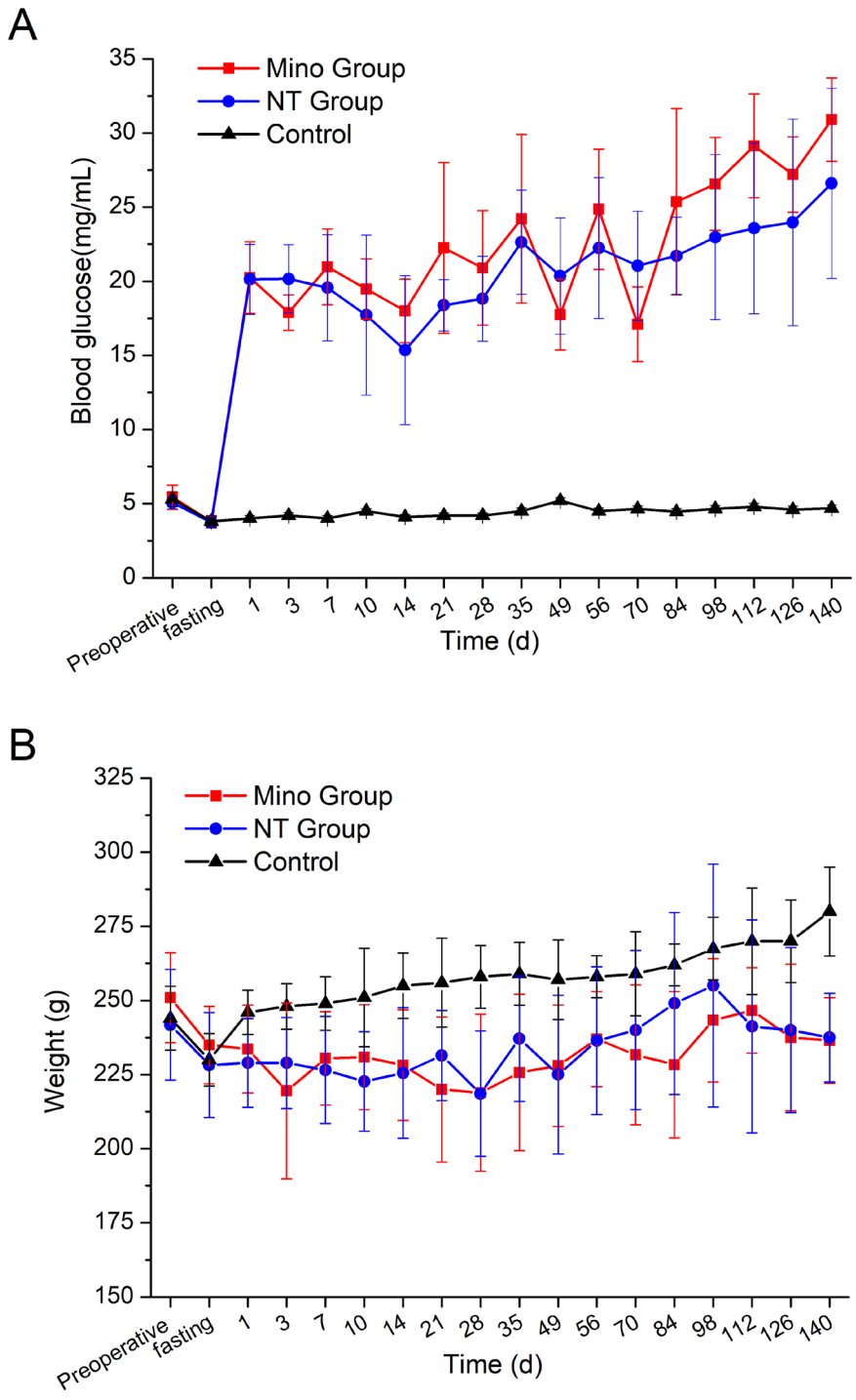

Figure 7. Blood glucose values. (**A**) and bodyweights (**B**) of rats in each group throughout the experiment (*n* = 10).

amplitudes were induced in Wistar rats four months after the induction of DR. Our study showed that dark-adapted a-wave and b-wave amplitudes decreased to varying extents beginning one month after the onset of diabetes. These reductions differed significantly from the amplitudes in the blank group, suggesting damage to rod cells in diabetic rats. The dark-adapted amplitudes tended to decrease in the treated eyes of the Mino group compared with the blank group. However, this difference was not statistically significant, presumably because of the small sample size and short follow-up duration. DR rats showed abnormal light-adapted amplitudes three months after the onset of diabetes, suggesting changes in cone cells. Malechka's findings suggested that the changes in retinal function were related to the reduction of rhodopsin in photoreceptors in diabetic rats [17], which may explain why the abnormal dark-adapted amplitudes appeared earlier compared with light-adapted amplitudes.

The main pathological mechanism of DR involves long-term high glucose exposure and endocrine dysfunction, which cause a decrease in perivascular cells, an increase in endothelial cells, and the thickening of basement membrane; these changes result in ischemia onset within retinal capillaries. Long-term ischemia and hypoxia cause retinal cells to secrete vascular growth factors (e.g., hypoxia-inducible factor-1 [HIF-1], vascular endothelial growth factor [VEGF], and placenta growth factor [PIGF]) to cause neovascularization. Dark-adapted OPs originate from the activity of the inhibitory feedback loop in the inner plexiform layer; this

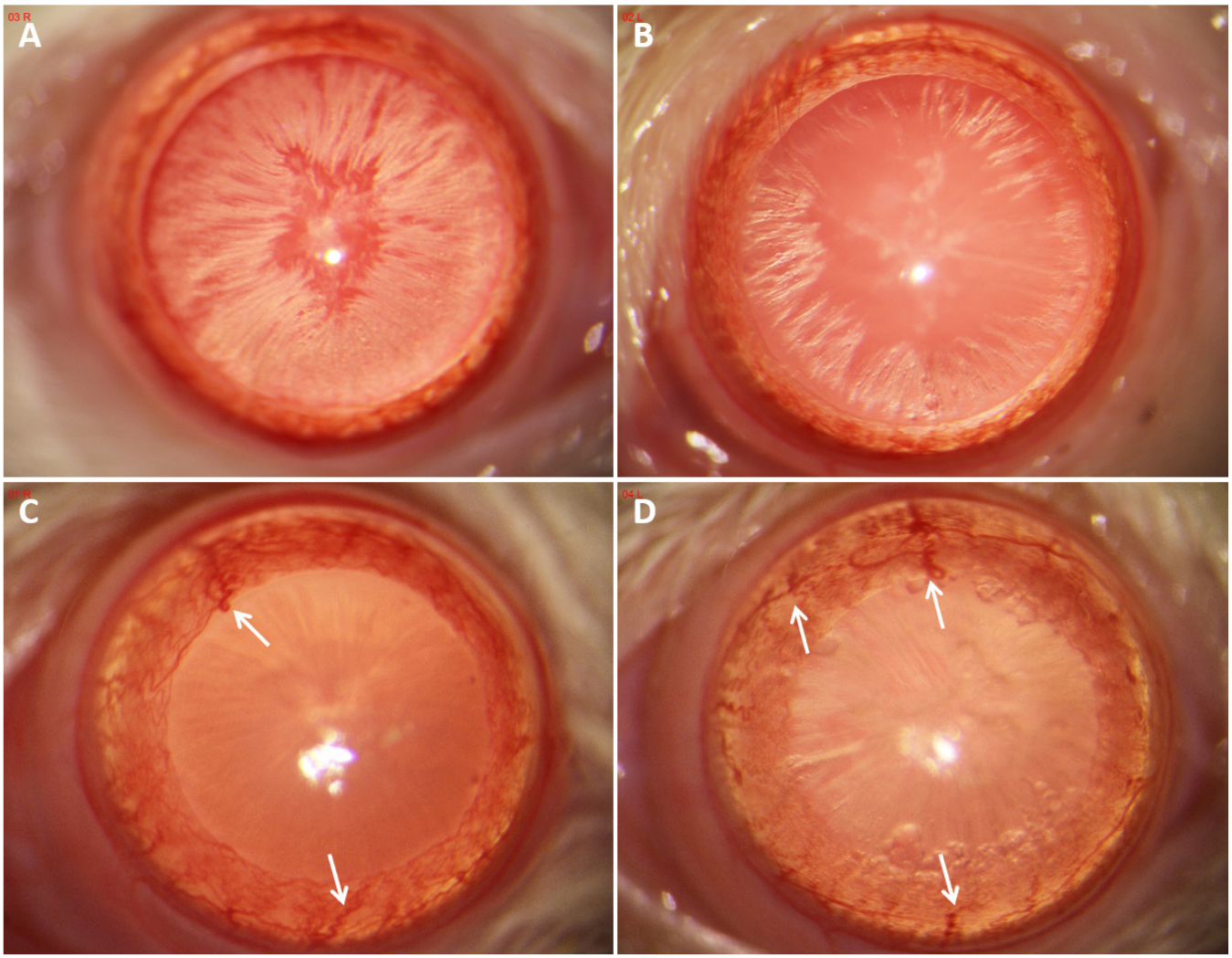

Figure 8. Photographs of the eye anterior segment in rats in the NT group (**A**, **C**) and Mino group (**B**, **D**) at one and three months after beginning the eye drop administration. A and B show cataract development in diabetic rats at one month after beginning the eye drop administration. **C** and **D** show iris vessel proliferation, thickening, and tortuosity (white arrows) three months after beginning the eye drop administration.

Table 4. Mean retinal thicknesses (mm) measured by OCT at 1, 2, and 3 months after eye drop administration.

Time	Layer	Mino-OD	Mino-OS	NT group	Control group
1 m	Whole layer	206.63±9.84	205.90±9.89	204.45±7.95	211.93±18.12
	GCIPL	77.83±6.72	75.29±6.35	74.94±6.45	82.70±6.08
		n=8	n=8	n=9	n=10
2 m	Whole layer	203.94±8.75	202.67±10.33	202.56±7.08	209.23±17.57
	GCIPL	76.57±7.24	74.07±5.85	73.88±7.24	82.72±5.76
		n=6	n=7	n=5	n=10
3 m	Whole layer	203.39±10.72	201.42±9.83	199.24±10.75	212.55±17.54
	GCIPL	75.83±6.37	72.42±5.99	71.47±5.10	81.92±5.64
		n=3	n=4	n=4	n=10

GCIPL, ganglion cell inner plexiform layer (distance from internal limiting membrane to inner plexiform layer); n, number of animals per group at each time point.

Table 5. Results of each ERG program at 1, 2, 3, and 4 months after administration of eye drops.

Program	Time	Wave	Mino-OD	Mino-OS	NT group	Control group
Dark-adapted 0.01 ERG	1 m	b-wave (μV)	60.54±6.49	54.36±17.22	55.63±23.68*	86.53±15.61
	2 m	b-wave (μV)	62.24±19.63	56.44±5.51	54.98±19.51*	82.13±8.91
	3 m	b-wave (μV)	58.70±18.25	55.80±13.35	53.99±11.73**	83.80±9.97
	4 m	b-wave (μV)	55.30±13.11	53.95±2.47	50.43±13.52**	85.59±10.93
Dark-adapted 3.0 ERG	1 m	a-wave (μV)	40.09±15.78	38.72±8.98	36.51±9.68	45.32±7.96
		b-wave (μV)	90.80±11.88	78.19±12.13	79.59±16.27*	107.05±32.44
	2 m	a-wave (μV)	36.27±6.01	32.87±4.18	31.14±9.48	38.55±4.65
		b-wave (μV)	103.09±38.49	82.03±13.52	81.97±26.70	108.7±10.73
	3 m	a-wave (μV)	35.80±8.07	34.77±4.15	31.40±16.84	36.10±5.57
		b-wave (μV)	79.89±12.06	70.97±11.51	65.37±20.32**	105.77±10.59
	4 m	a-wave (μV)	36.27±17.25	31.57±10.62	30.50±5.24	36.50±8.15
		b-wave (μV)	88.05±12.08	82.69±10.10	74.60±7.28***	109.47±6.03
Dark-adapted 3.0 oscillatory potential	1 m	OS_2 (μV)	48.67±15.39	45.38±11.16	46.63±16.73	61.12±19.06
	2 m	OS_2 (μV)	43.55±15.43	36.79±16.18	36.78±15.22*	61.33±17.67
	3 m	OS_2 (μV)	42.33±6.68	37.16±18.10	35.48±16.46*	60.88±19.34
	4 m	OS_2 (μV)	41.08±9.51	36.40±11.95	33.08±7.05*	61.50±18.27
Light-adapted 3.0 ERG	1 m	a-wave (μV)	2.49±0.91	2.87±0.62	2.66±0.40	2.61±1.38
		b-wave (μV)	23.80±5.79	22.79±4.30	22.58±3.03	22.13±6.45
	2 m	a-wave (μV)	2.34±0.75	2.52±0.56	2.60±0.43	2.75±0.90
		b-wave (μV)	19.23±3.42	18.07±3.06	18.00±6.21	21.35±2.26
	3 m	a-wave (μV)	1.41±0.25	1.12±0.38	0.97±0.21**	2.27±1.17
		b-wave (μV)	14.08±3.86	13.90±1.39	13.83±0.76***	19.43±1.96
	4 m	a-wave (μV)	0.93±0.27	0.74±0.57	0.64±0.02***	2.28±0.62
		b-wave (μV)	12.10±1.74	11.42±1.49	11.10±0.82***	22.05±2.13

Program	Time	Wave	Mino-OD	Mino-OS	NT group	Control group
Light-adapted Fare ERG	1 m	P1-N1 (ms)	16.59±2.20	17.09±3.01	16.49±2.42	15.37±2.05
		P1-N1 (μV)	4.26±0.70	3.93±1.32	3.93±1.10	4.47±1.54
	2 m	P1-N1 (ms)	17.60±0.35	18.05±0.64	18.74±2.95	16.88±1.80
		P1-N1 (μV)	3.83±1.25	3.40±0.35	3.78±1.33	4.40±0.73
	3 m	P1-N1 (ms)	17.30±2.04	17.80±4.35	18.27±2.52**	14.18±1.25
		P1-N1 (μV)	3.67±0.80*	2.63±0.42	2.20±1.04**	4.20±1.16
	4 m	P1-N1 (ms)	16.88±2.60	18.55±0.70	20.05±3.83*	15.20±0.71
		P1-N1 (μV)	3.22±1.24	2.55±0.86	2.48±0.63*	5.05±1.61

*p<0.05;**p<0.01; ***p<0.001. There was statistical significance between the control group and NT group.

Molecular Vision 2022; 28:460-479 <http://www.molvis.org/molvis/v28/460>

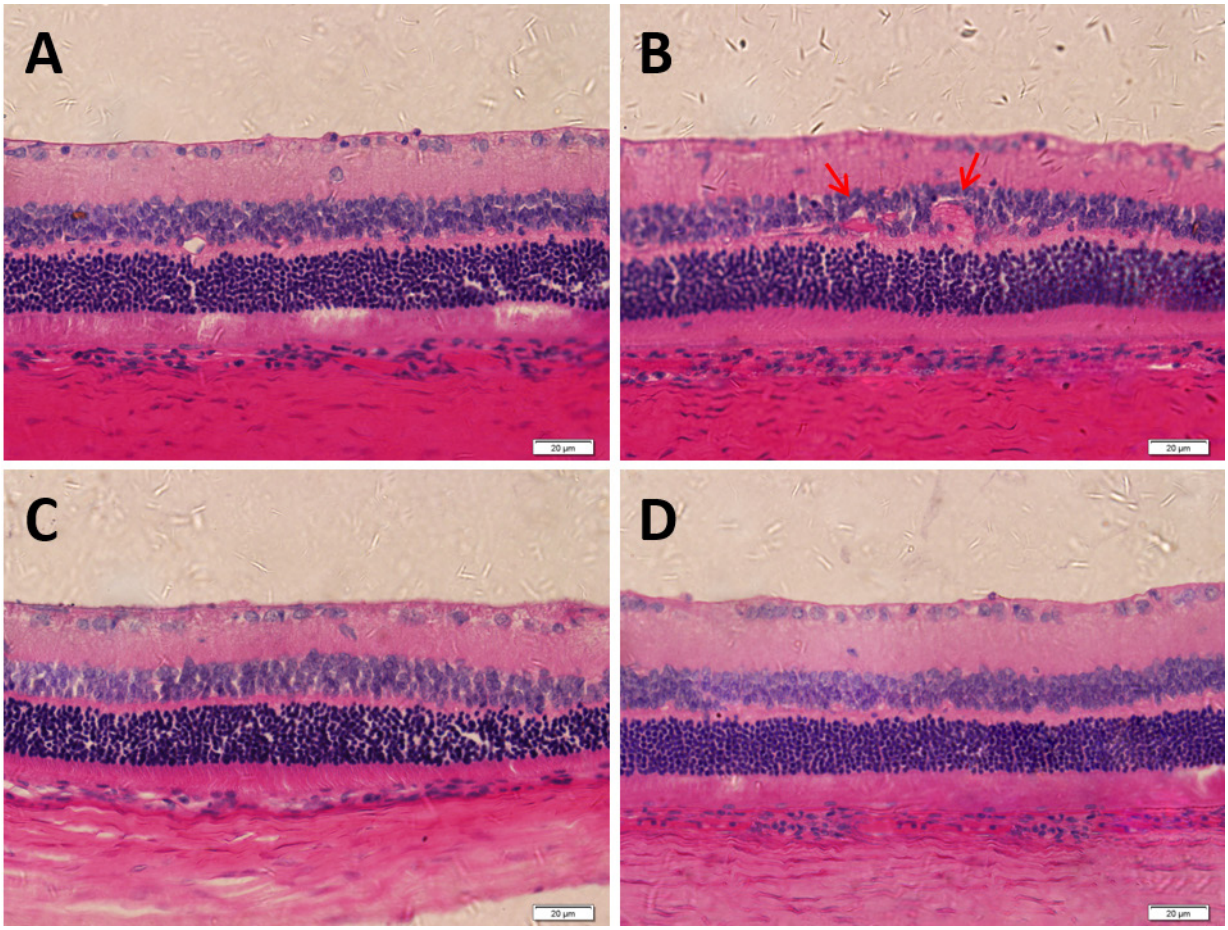

Figure 9. HE staining images of rat retinas in each group at four months after beginning the eye drop administration. **A**: Blank control group; **B**: Right eye of NT group; **C**: Right eye of Mino group; **D**: Fellow eye of Mino group. The red arrow in B indicates abnormal dilated retinal vessels. Scale bar: 20 μm.

measurement reflects retinal microcirculation. Our results showed that the OS_2 amplitude of the OPs in DR rats at two months after the onset of diabetes significantly differed compared with the control group; this finding suggested that the retinal microcirculation system was abnormal in diabetic rats. Importantly, the OS_2 amplitude was slightly greater in the Mino group than in the NT group, which suggests that Mino had an intervention effect on the microvascular system in the DR rats. Furthermore, BRB permeability tests suggested that Mino protected against the enhancement of BRB permeability caused by DR. Flat-mounted retina analyses showed that Mino had a protective effect on DR blood vessels. Previous studies [18,19] suggested that Mino mediated an anti-angiogenic effect by inhibiting VEGF-induced vascular smooth muscle cell migration. Doxycycline, which exhibits a structure similar to that of Mino, can induce membrane expression of VE-cadherin on endothelial cells and prevent vascular hyperpermeability [20]; it can also inhibit choroidal neovascularization [21]. Vincent [22] reported that Mino can prevent retinal capillary degeneration in diabetes. Overall, Mino has a protective effect on retinal vessels in DR rats.

In this study, we used OCT to observe retinal morphology and measure retinal thickness in experimental rats. OCT analyses showed that the overall retinal thickness and GCIPL thickness in DR rats gradually decreased, such that the measurements significantly differed from the blank control group. In histopathological analysis, Aizu [16] reported that the thicknesses of the overall retina, IPL, and photoreceptor segment layer (PSL) in SD rats decreased one month after the onset of diabetes, compared with those measurements in normal rats. Our histopathological analyses showed that the GCL thickness was reduced in DR rats compared with normal rats; moreover, the number of ganglion cells decreased in DR rats. However, we did not statistically analyze retinal thickness because of the small sample size. We found that DR rats developed retinal vasodilation and retinal structural

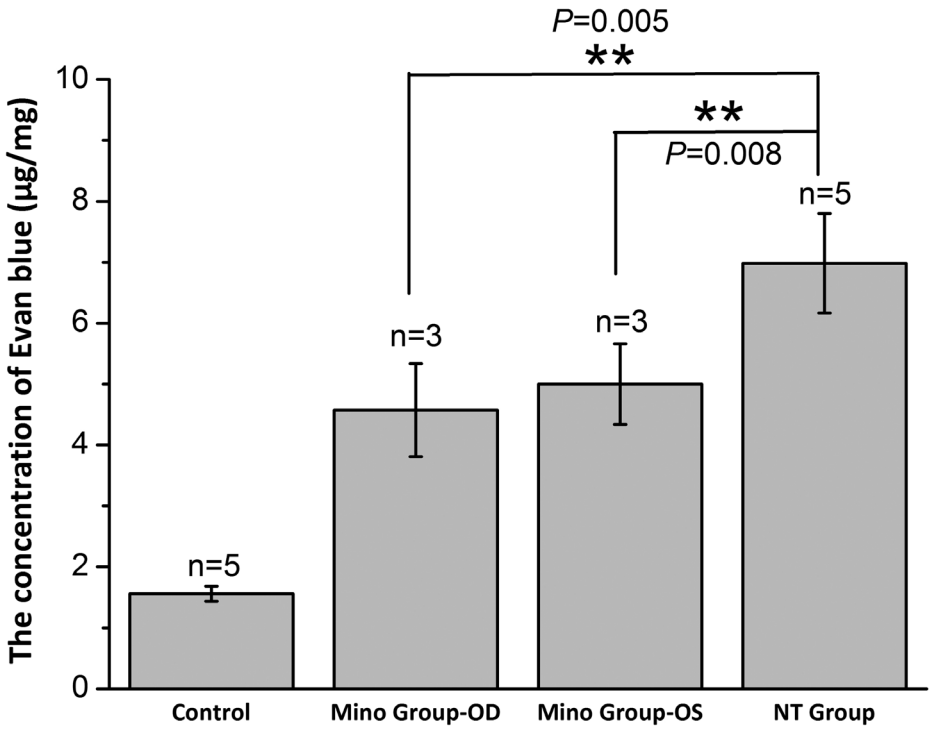

Figure 10. Evans blue content in the rat retinas of each group. ** Indicates $p < 0.01$.

disorders. The OCT analysis showed that retinal thickness was reduced in the Mino group at one month after the onset of diabetes, but this rate of thinning was slower than the rate in the NT group. Histopathological observations of morphology revealed no differences between the treated and fellow eyes in the Mino group. However, the number of ganglion cells was greater in the treated eyes in the Mino group than in the NT group. These findings indicate that Mino can inhibit retinal atrophy in DR rats.

This study did not investigate the mechanism by which Mino affects DR. Previous studies have suggested that Mino delays DR development by means of an anti-inflammatory effect. Mino reduced proinflammatory cytokine expression, microglial activation, and caspase-3 activation in rats with DR [2]. Moreover, Mino reduced inflammation and cell apoptosis by inhibiting MMP-2 and MMP-9 in STZ-induced diabetic rats [23]. Some researchers have studied the anti-inflammatory effect of Mino from the perspective of histone

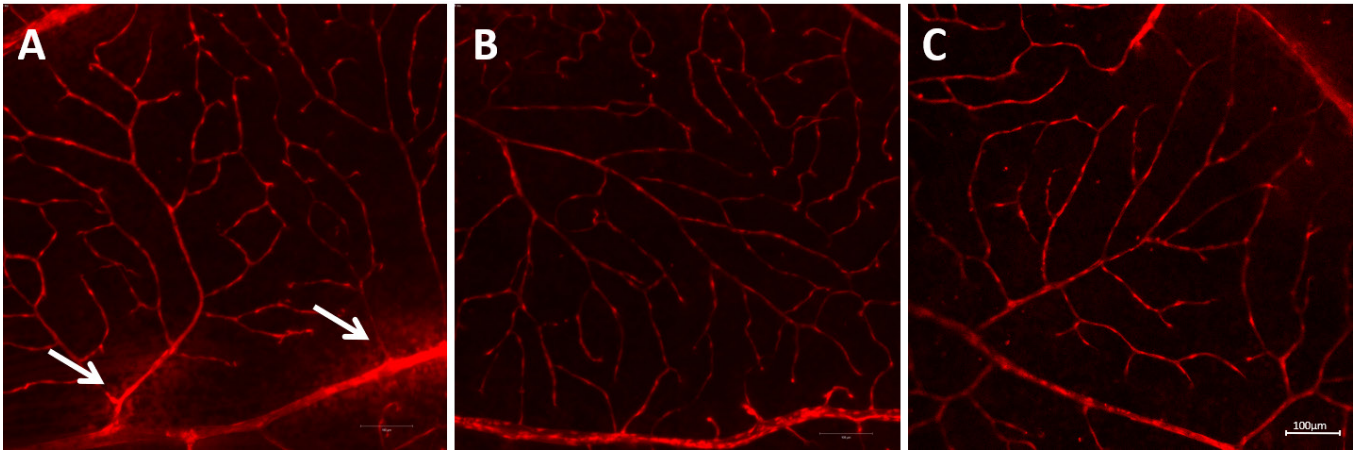

Figure 11. Retinal vessels in each group at four months after beginning the eye drop administration. **A**: Right eye in the NT group; **B**: Right eye in the Mino group; **C**: Left eye in the Mino group. The white arrow in A indicates vascular leakage. Scale bar: 100 μm.

modification. Wang et al. [24] found that the enhancement of histone acetylation in Müller cells played a critical regulatory role in the inflammatory response during diabetic conditions. Thus, the inhibition of histone acetylation by Mino might be important for its beneficial effects on DR. Wenjun [25] reported that the alteration of some histone methylation levels was associated with the development of DR in rodents; the beneficial effect of Mino on the retinas of diabetic rodents was partially mediated by its ability to normalize the alterations in histone methylation levels.

In conclusion, the topical delivery of Mino had protective effects on the retinal function, retinal vascular, retinal thickness, and morphology of the DR rats. These findings provide an experimental basis for the clinical application of Mino eye drops.

ACKNOWLEDGMENTS

Ethical approval: All animal procedures and numbers (42 rats) were approved by the Wenzhou Medical University Ethics Committee. This work was supported by Zhejiang Provincial Natural Science Foundation of China [grant number is LQ18H180004].

REFERENCES

1. Eid S, O'Brien P, Hinder L, Hayes J, Mendelson F, Zhang H, Narayanan S, Abcouwer S, Brosius F, Pennathur S, Savelieff M, Feldman E. Differential effects of minocycline on microvascular complications in murine models of type 1 and type 2 diabetes. J Transl Sci. 2021;7.
2. Krady JK, Basu A, Allen CM, Xu Y, LaNoue KF, Gardner TW, Levison SW. Minocycline reduces proinflammatory cytokine expression, microglial activation, and caspase-3 activation in a rodent model of diabetic retinopathy. Diabetes 2005; 54:1559-65. [PMID: 15855346].
3. Chen W, Zhao M, Zhao S, Lu Q, Ni L, Zou C, Lu L, Xu X, Guan H, Zheng Z, Qiu Q. Activation of the TXNIP/NLRP3 inflammasome pathway contributes to inflammation in diabetic retinopathy: a novel inhibitory effect of minocycline. Inflamm Res 2017; 66:157-66. [PMID: 27785530].
4. Vincent JA, Susanne M. Inhibition of caspase-1/interleukin-1beta signaling prevents degeneration of retinal capillaries in diabetes and galactosemia. Diabetes 2007; 56:224-[PMID: 17192486].
5. Cukras CA, Petrou P, Chew EY, Meyerle CB, Wong WT. Oral minocycline for the treatment of diabetic macular edema (DME): results of a phase I/II clinical study. Invest Ophthalmol Vis Sci 2012; 53:3865-74. [PMID: 22589436].
6. Wu W, He Z, Zhang Z, Yu X, Song Z. Intravitreal injection of rapamycin-loaded polymeric micelles for inhibition of ocular inflammation in rat model. Int J Pharm 2016; 513:238-246. [PMID: 27609662].
7. Saivin S, Houin G. Clinical Pharmacokinetics of Doxycycline and Minocycline. Clin Pharmacokinet 1988; 15:355-66. [PMID: 3072140].
8. Hollborn M, Wiedemann P, Bringmann A, Kohen L. Chemotactic and cytotoxic effects of minocycline on human retinal pigment epithelial cells. Invest Ophthalmol Vis Sci 2010; 51:2721-9. [PMID: 20019360].
9. Hughes PM, Olejnik O, Chang-Lin JE, Wilson CG. Topical and systemic drug delivery to the posterior segments. Adv Drug Deliv Rev 2005; 57:2010-32. [PMID: 16289435].
10. Lee VH, Robinson J. Topical ocular drug delivery: recent developments and future challenges. J Ocul Pharmacol 1986; 2:67-108. [PMID: 3332284].
11. Rehany U, Ishii Y, Lahav M, Rumelt S. Ultrastructural Changes in Corneas of Diabetic Patients. Cornea 2000; 19:534-8. [PMID: 10928773].
12. Maurice DM. Drug Delivery to the Posterior Segment from Drops. Surv Ophthalmol 2002; 47:S41-52. [PMID: 12204700].
13. Olsen TW, Edelhauser HF, Lim JI, Geroski DH. Human scleral permeability. Effects of age, cryotherapy, transscleral diode laser, and surgical thinning. Invest Ophthalmol Vis Sci 1995; 36:1893-903. [PMID: 7543465].
14. Falavarjani KG, Nguyen QD. Adverse events and complications associated with intravitreal injection of anti-VEGF agents: a review of literature. Eye (Lond) 2013; 27:787-94. [PMID: 23722722].
15. Li Q, Zemel E, Miller B, Perlman I. Early retinal damage in experimental diabetes: electroretinographical and morphological observations. Exp Eye Res 2002; 74:615-25. [PMID: 12076083].
16. Aizu Y, Oyanagi K, Hu J, Nakagawa H. Degeneration of retinal neuronal processes and pigment epithelium in the early stage of the streptozotocin-diabetic rats. Neuropathology 2010; 22:161-70. [PMID: 12416555].
17. Malechka VV, Moiseyev G, Takahashi Y, Shin Y, Ma JX. Impaired Rhodopsin Generation in the Rat Model of Diabetic Retinopathy. Am J Pathol 2017; 187:2222-2231. [PMID: 28734946].
18. Yao JS, Shen F, Young WL, Yang GY. Comparison of doxycycline and minocycline in the inhibition of VEGF-induced smooth muscle cell migration. Neurochem Int 2007; 50:524-30. [PMID: 17145119].
19. Yao JS. Minocycline Exerts Multiple Inhibitory Effects on Vascular Endothelial Growth Factor–Induced Smooth Muscle Cell Migration The Role of ERK1/2, PI3K, and Matrix Metalloproteinases. Circ Res 2004; 95:364-71. [PMID: 15256478].
20. Fainaru O, Adini I, Benny O, Bazinet L, Folkman J. Doxycycline induces membrane expression of VE-cadherin on endothelial cells and prevents vascular hyperpermeability. FASEB J 2008; 22:3728-[PMID: 18606869].
21. Cox CA, Amaral J, Salloum R, Guedez L, Carper DA. Doxycycline's Effect on Ocular Angiogenesis: An In Vivo Analysis. Ophthalmology 2010; 117:1782-91. [PMID: 20605212].

22. Vincent JA, Mohr S. Inhibition of caspase-1/interleukin-1beta signaling prevents degeneration of retinal capillaries in diabetes and galactosemia. Diabetes 2007; 56:224-[PMID: 17192486].

23. Bhatt LK, Addepalli V. Attenuation of diabetic retinopathy by enhanced inhibition of MMP-2 and MMP-9 using aspirin and minocycline in streptozotocin-diabetic rats. Am J Transl Res 2010; 2:181-9. [PMID: 20407607].

24. Wang LL, Hong C, Huang K, Ling Z. Elevated histone acetylations in Müller cell contribute to inflammation: A novel inhibitory effect of minocycline. Glia 2012; 60:1896-905. [PMID: 22915469].

25. Wang W, Sidoli S, Zhang W, Wang Q, Wang L, Jensen ON, Guo L, Zhao X, Zheng L. Abnormal levels of histone methylation in the retinas of diabetic rats are reversed by minocycline treatment. Sci Rep 2017; 7:45103-[PMID: 28338045].

Articles are provided courtesy of Emory University and the Zhongshan Ophthalmic Center, Sun Yat-sen University, P.R. China. The print version of this article was created on 21 December 2022. This reflects all typographical corrections and errata to the article through that date. Details of any changes may be found in the online version of the article.